Flexible Lead-Free Piezoelectric Composite Materials for Energy Harvesting Applications

Stuber, Vincent L.; Deutz, Daniella B.; Bennett, James; Cannel, David; de Leeuw, Dago M.; van der Zwaag, Sybrand; Groen, Pim

DOI
10.1002/ente.201800419

Publication date
2019

Document Version
Final published version

Published in
Energy Technology

Citation (APA)
Stuber, V. L., Deutz, D. B., Bennett, J., Cannel, D., de Leeuw, D. M., van der Zwaag, S., & Groen, P. (2019). Flexible Lead-Free Piezoelectric Composite Materials for Energy Harvesting Applications. *Energy Technology*, *7*(1), 177-185. https://doi.org/10.1002/ente.201800419

DOI: 10.1002/ente.201800419

Flexible Lead-Free Piezoelectric Composite Materials for Energy Harvesting Applications

Vincent L. Stuber,*[a] Daniella B. Deutz,[b] James Bennett,[c] David Cannel,[c] Dago M. de Leeuw,[a] Sybrand van der Zwaag,[a] and Pim Groen*[a, d]

Vibrational piezoelectric energy harvesters are being investigated to replace batteries in embedded sensor systems. The energy density that can be harvested depends on the figure of merit, $d_{33}g_{33}$, where d_{33} and g_{33} are the piezoelectric charge and voltage coefficient. Commonly used piezoelectric materials are based on inorganic ceramics, such as lead zirconium titanate (PZT), as they exhibit high piezoelectric coefficients. However, ceramics are brittle, leading to mechanical failure under large cyclic strains and, furthermore, PZT is classified as a Substance of Very High Concern (SVHC). To circumvent these drawbacks, we fabricated quasi 1–3 potassium sodium lithium niobate (KNLN) ceramic fibers in a flexible polydimethylsiloxane (PDMS) matrix. The fibers were aligned by dielectrophoresis. We demonstrate for the structured composites values of $d_{33}g_{33}$ approaching 18 pm^3J^{-1}, comparable to that of state-of-the-art ceramic PZT. This relatively high value is due to the reduced inter-particle distance in the direction of the electric field. As a confirmation, the stored electrical energy for both material systems was measured under identical mechanical loading conditions. The similar values for KNLN/PDMS and PZT demonstrate that environmentally friendly, lead-free, mechanically compliant materials can replace state-of-the-art environmentally-less-desirable ceramic materials in piezoelectric vibrational energy harvesters.

1. Introduction

More and more embedded sensor systems are employed in our daily lives, such as medical implants, structural health monitoring in civil infrastructure, and the internet of things. These systems are normally powered by batteries, which need to be replaced or recharged, pollute the environment once thrown away, and are in general volumetrically the largest component of the harvester. One way of dealing with this drawback, is to eliminate the battery and use energy harvesting instead; extracting energy from the surrounding environment and in-situ converting it into electrical energy.[1,2]

Depending on the application, our natural environment offers several forms of energy to be converted, such as solar power, wind energy, flowing water and mechanical energy. Here we focus on harvesting mechanical energy, such as vibrations from machines, repetitive body motion or small scale impact.[3,4] Possible methods that can be used are electrostatic or electromagnetic induction and piezoelectricity.[5,6] Current emphasis is on piezoelectric materials as they can directly convert mechanical energy into electrical energy, leading to harvesters with high energy density at small volume, while they are also easy to integrate into systems due to their design flexibility.[7,8]

The output of a vibrational harvester strongly depends on the boundary conditions of the applied mechanical load. Numerous mechanical designs are used to optimize the strain per unit of load, such as bimorph cantilevers, unimorph diaphragms and cymbal transducers, but a high strain is a device attribute and does not automatically imply a high energy density. In order to compare the performance of piezoelectric materials themselves, the product of the piezoelectric charge coefficient, d_{33}, and the piezoelectric voltage coefficient, g_{33}, is being used.[9,10] This figure of merit, $d_{33}g_{33}$, is a measure of the energy density per unit volume that can be harvested. We note that $d_{33}g_{33}$ is equal to $d_{33}^2/\varepsilon_r\,\varepsilon_0$, where ε_0 is the permittivity of vacuum and ε_r is the relative dielectric constant.

Not surprisingly, therefore, commonly used piezoelectric materials are based on inorganic ceramics, such as lead zirconium titanate (PZT), due to the high values of the piezoelectric coefficients, *i.e.* $d_{33}g_{33}$ is about 10–22 pm^3J^{-1}, and high Curie temperature, *i.e.* T_C is about 160–370 °C. However, PZT and related materials have two drawbacks.[11–13] Firstly, ceramics are brittle, leading to mechanical failure under large cyclic strains. Secondly, due to the presence of Pb, the commonly used inorganic piezoelectric material PZT is classified as a Substance of Very High Concern (SVHC) according to the European Community REACH regulation 1907/2006/EEC. To circumvent these drawbacks, alternative non-toxic piezoelectric materials are being investigated. Piezoelectric polymers, such as poly(vinylidine-fluoride) (PVDF) and its copolymers, have the advantage of being flexible. This implies that large cyclic strains can be repetitively applied without deterioration of the reliability. However, the application of piezoelectric polymers is hampered

[a] V. L. Stuber, D. M. de Leeuw, S. van der Zwaag, P. Groen
Delft University of Technology, Kluyverweg 1, 2629 HS Delft, The Netherlands
E-mail: V.L.Stuber@tudelft.nl
W.A.Groen@tudelft.nl
[b] D. B. Deutz
University of Southern Denmark, Campusvej 55, 5230 Odense, Denmark
[c] J. Bennett, D. Cannel
CeramTec, Ruabon, UK
[d] P. Groen
TNO, Holst Centre, 5606 KN Eindhoven, The Netherlands

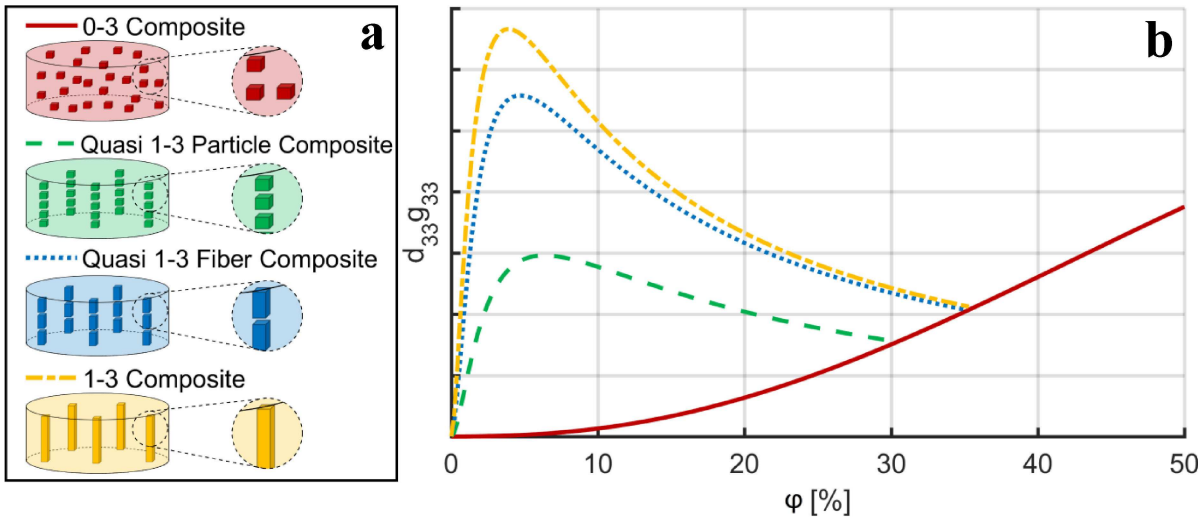

Figure 1. (a) Representative connectivity schemes of piezoelectric composite materials. (b) As an illustration, we present the energy harvesting figure of merit, $d_{33}g_{33}$, as a function of volume fraction, φ, of piezoelectric filler. The lines are calculated using, arbitrarily, the Yamada model[20] for a random composite, and the Van den Ende model[21] and the Bowen model[29] to calculate d_{33} and ε_r, respectively, for structured composites. Model parameters were kept constant as much as possible, to arrive at a qualitative picture in arbitrary units. The piezoelectric properties of the various 1–3 composites are anisotropic. Here we present the longitudinal piezoelectric constants.

due to their limited energy harvesting potential, as $d_{33}g_{33}$ is only 5 $pm^3\,J^{-1}$. Furthermore, they exhibit a low Curie temperature of about 100 °C, and require a high coercive field for poling of 60 $MV\,m^{-1}$.[14,15] Here we demonstrate that piezoelectric composites are a worthwhile alternative.

Piezoelectric composites combine an (inert) polymeric matrix with a piezoelectric ceramic filler.[16–18] The polymeric matrix yields the mechanical flexibility. At a low volume fraction of piezoelectric filler, up to about 10 percent, the Young's modulus of a piezoelectric composite is comparable to that of the polymeric matrix. The ceramic filler renders the composite piezoelectric. The charge coefficient, d_{33}, increases with filler volume fraction. More importantly however, the charge coefficient strongly depends on the connectivity, defined as the number of dimensions in which a phase is self-connected.[19] For a composite containing two phases, there are sixteen connectivity patterns, which range from 0–0, where neither phase is self-connected, to 3–3, where each phase is self-connected in three dimensions. In this convention, the first digit refers to the active piezoelectric ceramic phase, while the second digit refers to the polymeric matrix. Representative connectivity schemes are presented in Figure 1a. A 0–3, or random, composite is easy to fabricate. However, at low volume fraction of ceramic particles, the electric field is confined in the low dielectric constant polymeric matrix. There is no electric field over the disconnected piezoelectric particles and, therefore, at low volume fractions a random composite is hardly piezoelectric.[20,21] On the other hand, a 1–3 composite contains continuous ceramic pillars. The composite therefore exhibits larger piezoelectric coefficients, but the main drawback is the difficult manufacturing route, as it entails cutting and refilling ceramics.[22,23] A method to combine the easy manufacturing of the 0–3 composite with the piezoelectric properties of the 1–3 composite is to align discrete ceramic particles in the polymeric matrix while it is in a low viscosity state, obtaining quasi 1–3, or structured, particle composites. By doing this, the inter-particle distance in the field direction is reduced significantly. The smaller the inter-particle distance, the higher the electromechanical coupling. In practice this can be realized in two ways. Firstly, the filler particles can be aligned, the distance between the filler particles is then smaller than in a random composite. Secondly, the number of interconnects can be minimized, for instance by the use of high aspect ratio fibers instead of spherical particles. The limiting case is then again a 1–3 composite. Consequently, at low volume fractions, the improved connectivity of the filler particles rapidly improves d_{33} with volume fraction. At higher volume fractions, the d_{33} increases less and less.[21,24,25]

Contrary to the charge coefficient, the dielectric constant, ε_r, experiences only a marginal increase due to alignment of the particles. The dielectric constant is dominated by that of the polymeric matrix, hardly depends on the microstructure and increases approximately linearly with the volume fraction of ceramic particles. As an illustration we calculated the figure of merit, $d_{33}g_{33}$, as a function of filler volume fraction for 0–3, 1–3 and quasi 1–3 composites. There are various models that describe ε_r and d_{33} as a function of filler volume fraction.[20,21,26–29] All these models give comparable values.[30] We arbitrarily used the Yamada model for random composites, and the Van den Ende model (for d_{33}) in combination with the Bowen model (for ε_r) for the structured composites. Using these models, the lines in Figure 1b are calculated. The product $d_{33}g_{33}$ depends on numerous parameters, such as the dielectric constant of matrix and filler, bulk piezoelectric charge coefficient, poling efficiency, aspect ratio of particles and fibers, and the inter-particle distance. The parameters were kept constant as much as possible to give the qualitative

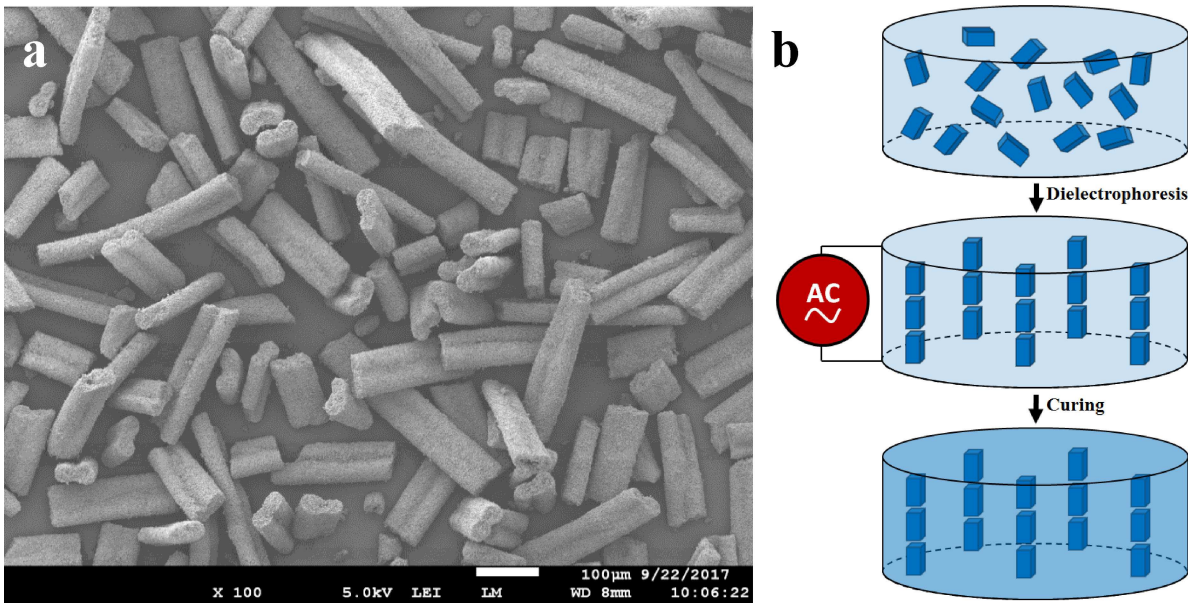

Figure 2. (a) SEM micrograph of the sintered KNLN fibers. (b) Schematic representation of the alignment of the piezoelectric fibers using dielectrophoresis.

representation of Figure 1b. We note that, at high volume fraction, the predicted value of $d_{33}g_{33}$ of structured 1–3 composites is lower than that of random 0–3 composites. This counterintuitive behaviour is an artefact of the theoretical models; for instance at high volume fraction the dielectric constant is over-estimated. It has been experimentally shown that at high volume fraction alignment is not advantageous for the piezoelectric coefficients.[31] Therefore, in Figure 1b, at high volume fraction all models should converge to that of the random 0–3 composite.

For a random composite the value of $d_{33}g_{33}$ is small, and monotonically increases with filler volume fraction, as shown in Figure 1b. As expected, a structured composite exhibits a higher value in the low volume fraction region. The figure of merit peaks at about 5–10 vol % due to the steep increase of the charge coefficient at low filler volume fractions. The maximum value of $d_{33}g_{33}$ increases with decreasing inter-particle distance, from quasi 1–3 particle composites, through quasi 1–3 fiber composites,[32] to 1–3 composites. Figure 1b clearly shows that, due to the decreased inter-particle distance, the fiber composites are preferred over particle composites. Composites for energy harvesting should preferably comprise a low volume fraction of aligned piezoelectric fibers in polymeric matrix with a low dielectric constant.

Here we fabricate state-of-the-art piezoelectric quasi 1–3 fiber composite materials. As an environmentally friendly, lead free ceramic filler we used aligned $K_{0.485}Na_{0.485}Li_{0.03}NbO_3$ (KNLN) fibers. Polydimethylsiloxane (PDMS) is used as the polymeric matrix, since it has a low dielectric constant. The Young's modulus of a few MPa leads to mechanically flexible composites, which can handle multiple cyclic strains without affecting the reliability. The KNLN fibers are aligned through dielectrophoresis, which entails the application of an AC electric field while the polymeric PDMS matrix is still in its liquid state.[29,33] After alignment, to minimize the inter-particle distance, the PDMS is cured to fix the microstructure. The fabricated piezoelectric fiber composites are fully characterized as a function of filler volume fraction. To compare the fiber composites with state-of-the-art PZT, we measured the output energy in the simple boundary condition of a clamped disc. Although the output energy using this configuration is limited, this is the only reliable way to compare piezoelectric materials.[10]

2. Fabrication of Aligned KNLN/PDMS Fiber Composites

2.1. Preparation of KNLN fibers

Green $K_{0.485}Na_{0.485}Li_{0.03}NbO_3$ (KNLN) powder was obtained from CeramTec, Ruabon, UK, and calcined at 800 °C for 2 hours (heating rate of 1 °C min^{-1}) to decompose the starting oxides and to obtain a single phase material. Afterwards, the powder was milled using 10 mm yttria-stabilized ZrO_2 balls immersed in cyclohexane. The KNLN particles were mixed in a 20 wt % solution of cellulose acetate (M_N 30,000, Aldrich Chemistry) in acetone, with a volume ratio of KNLN particles to cellulose acetate of 1:1. The mixture was used to spin fibers using the wet spinning technique in a water coagulation bath. After spinning, the fibers were dried and sintered at 1050 °C for 1 hour (heating rate of 5 °C min^{-1}) in a closed Al_2O_3 crucible. To allow dielectrophoretic alignment, the fibers were broken into short fragments. An SEM micrograph, presented in Figure 2a, shows that the fibers have a kidney-like cross-sectional shape caused by evaporation of acetone. The fibers have a diameter of 27 µm by 54 µm and a

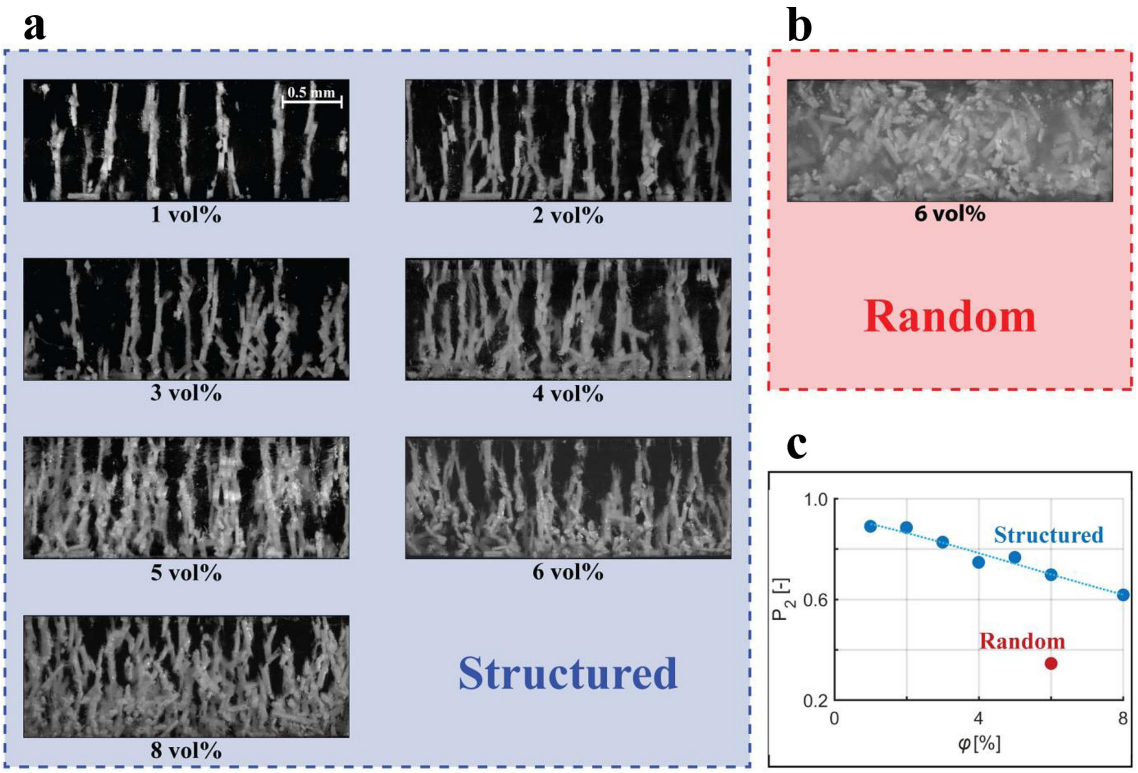

Figure 3. Microstructure of dielectrophoretically aligned KNLN fibers in a PDMS matrix. a) Optical micrographs of cross sections of structured composites as a function of volume fraction. b) Optical micrograph of the cross section of a random composite. c) Orientational order parameter, $\overline{P_2}$, as a function of volume fraction, φ. The dotted line is a guide for the eye.

length of about 150–200 μm, yielding an aspect ratio between 3 and 4.

2.2. Dielectrophoretic alignment of KNLN fibers

The fibers were mixed in two component polydimethylsiloxane (PDMS) (Sylgard 184, Dow Corning) with varying volume fraction (1–8 vol %) in a planetary speed mixer (DAC 150 FVZ, Hauschild, Germany). The slurry was degassed and poured into prefabricated holes punched into a Teflon sheet. The sheet was covered with two aluminum foils on both sides, acting as electrodes for dielectrophoresis, and clamped between two steel plates.

Dielectrophoresis has proven to be a well-suited technique to align a piezoelectric ceramic filler as the active phase, into a low dielectric polymeric matrix as passive phase.[21,24,25] The process is schematically depicted in Figure 2b. An AC electric field of 4 kV mm^{-1} was used. The alignment efficiency of dielectrophoresis can be obtained from the phase angle between the applied voltage and leakage current, which depends on frequency. The equivalent electrical circuit of the dielectrophoretic setup is basically a resistor, originating from the uncured polymeric part of the sample, in parallel with a capacitor, originating from the piezoelectric filler part of the sample. At high frequency the capacitor is shorted and there is no driving force for filler particles to align. On the other hand, at low frequencies the direct current through the uncured polymer matrix becomes dominant, reducing the effective electric field on the filler particles. The optimal frequency is obtained when the phase angle in the uncured composite slurry is 90°. The system then is almost purely capacitive, with minimal leakage current. Here, the frequency was varied from 1 mHz to 10 kHz. We obtained, at a frequency of 200 Hz, a maximum angle of about 83°–85°, close to the optimum obtainable angle of 90°.

After alignment, the composites were cured at 100 °C for 1.5 hours to permanently fix the fiber orientation. The AC field remained turned on to prevent sedimentation. The fiber alignment can be inferred from optical images of cross sections of the structured composites. Numerous cross sections of all the volume fractions where investigated. The optical images are identical, all samples fabricated are macroscopically homogeneous. To demonstrate the details of the microstructure, we present enlarged images of the full cross sections in Figure 3a. For all volume fractions investigated, *i. e.* 1–8 vol %, the fibers form clear bridges between the top and bottom electrode. However, the alignment decreases with increasing filler volume fraction. Furthermore, gravity effects cannot be fully suppressed; especially at high volume fraction the bottom part of the sample shows more fibers than the top part. To quantify the alignment of the KNLN fibers we extracted the orientational order parameter as the average of the second Legendre polynomial:[34]

$$\overline{P_2} = \overline{\frac{3}{2}\cos^2\beta - \frac{1}{2}} \quad (1)$$

where β is the angle between the fiber chain and the surface normal, which is equal to the direction of the applied electric field. The order parameter varies between 0 for isotropic materials to 1 for perfectly aligned fiber composites. The order parameter as a function of filler volume fraction is presented in Figure 1c and shows a monotonic decrease from 0.9 to 0.6 for volume fractions between 1–8 vol %. Apparently, at higher volume fractions, the fibers obstruct each other's rotation and lateral displacement, which hampers quasi-fibre formation.[35] As reference, a random composite has been prepared with 6 vol % filler. No electric field was applied and during curing the mold was turned upside down every 10 minutes to prevent sedimentation. The optical image of the cross section is presented in Figure 3b. The extracted order parameter is only 0.3, significantly lower than 0.6 for the structured composite, which shows that dielectrophoresis is a versatile method to align piezoelectric fibers in a polymeric matrix.

3. Piezoelectric Coefficients of Aligned KNLN/PDMS Composites

To make the ferroelectric materials and composites act piezoelectrically, poling is required. To that end, capacitors where fabricated by sputtering gold electrodes through a shadow mask on both sides of the composites with a sputter coater (Quorum Q300T, East Sussex, United Kingdom). We performed numerous poling experiments where the poling time, the poling temperature and the applied electric field was varied deliberately. The optimal conditions obtained were an electric field of 15 kV/mm, a temperature of 150 °C and a poling time of 5 minutes. Increase in the poling time did not lead to higher values of the piezoelectric constants of the present composites. We note that the conditions used for poling are in perfect agreement with reported poling studies on comparable KNLN/PDMS composites.[25,36] Subsequently, the composites were aged for at least 24 hours before measuring the piezoelectric constants.

Piezoelectric- and dielectric constants of the capacitors were measured as a function of volume fraction. Extracted data points are presented in Figure 4. Blue circles refer to structured quasi 1–3 fiber composites, and red squares refer to random 0–3 fiber composites. The dash-dotted lines are a guide for the eye, calculated with the same arbitrary models as used in Figure 1. The relative dielectric constant, ε_r, and the corresponding dielectric loss, $tan(\delta)$, as a function of filler volume fraction, φ, are shown in Figures 4a and 4b, respectively. The dielectric constant linearly increases with volume fraction due to the dielectric constant of the KNLN fiber being orders of magnitude larger than that of the PDMS matrix. The dielectric constant increases upon alignment, as commonly observed in dielectrophoretically aligned composites.[21,24,25,31] Meanwhile, in all cases the dielectric loss does not exceed 3 %, and slightly increases with alignment. The piezoelectric charge coefficient monotonically increases with volume fraction, shown in Figure 4c. Furthermore, the values strongly increase upon aligning the fibers. As the increase in charge coefficient is non-linear, the piezoelectric voltage coefficient, shown in Figure 4d, and $d_{33}g_{33}$, shown in Figure 4e, show a maximum at a volume fraction of only 3–6 vol %. The maximum value for $d_{33}g_{33}$ is 18 $pm^3 J^{-1}$, the value of which will be compared to classical bulk ceramics in the next section. To demonstrate the important role of the inter-particle distance, we include as the green triangles, data previously obtained for dielectrophoretically aligned quasi 1–3 KNLN/PDMS *particle* composites. The piezoelectric coefficients are in between those of random and aligned *fiber* composites, in perfect agreement with the qualitative picture of Figure 1. The same trend is supported by reported data on PZT composites,[32] which clearly demonstrates that piezoelectric properties can be optimized by using aligned fiber composites.

4. Comparison of Piezoelectric Materials

Table 1 gives an overview of a representative number of reported piezoelectric materials. The materials in the table range from bulk materials, through random composites and structured particle and fiber composites, to a 1–3 composite. The ceramic filler comprises lead titanate (PT), PZT and KNLN, and as polymeric matrix PDMS, polyurethane (PU) and epoxy are used. The entries are sorted by $d_{33}g_{33}$. The table shows that bulk ceramic materials typically have a high d_{33} value. However, the large dielectric constant severely limits the g_{33} values. Consequently, for bulk ceramics $d_{33}g_{33}$ varies from 2 to 22 $pm^3 J^{-1}$, where the state-of-the-art value is obtained with PZT507. On the other hand, composites exhibit lower values of d_{33}, but due to the low dielectric constant of the polymeric matrix, their g_{33} reaches state-of-the-art values up to 500 $mV m N^{-1}$. We note that the 1–3 composite from the table is an exception to this rule due to the high volume fraction and perfect alignment. This causes the d_{33} to be high while the g_{33} stays low, comparable to bulk ceramics.

As stated earlier, for composites the value of $d_{33}g_{33}$ strongly depends on the microstructure. Random composites are piezoelectric, especially at high volume fractions. However, the mechanical flexibility then is impaired. The value of d_{33} can be dramatically improved by aligning the ceramic filler. Due to the low dielectric constant of the composite, g_{33}, and therefore $d_{33}g_{33}$, peak at low volume fractions. The maximum value depends on the inter-particle distance, and therefore, aligned fiber composites are preferred over aligned particle composites. Table 1 shows that the highest value obtained with composites is 18 $pm^3 J^{-1}$ for structured KNLN fibers in PMDS. This value is comparable to state-of-the-art PZT ceramics. Additionally, due to the low volume fraction, structured composites remain mechanically flexible, which gives an additional degree of freedom to optimize a vibrational harvester.

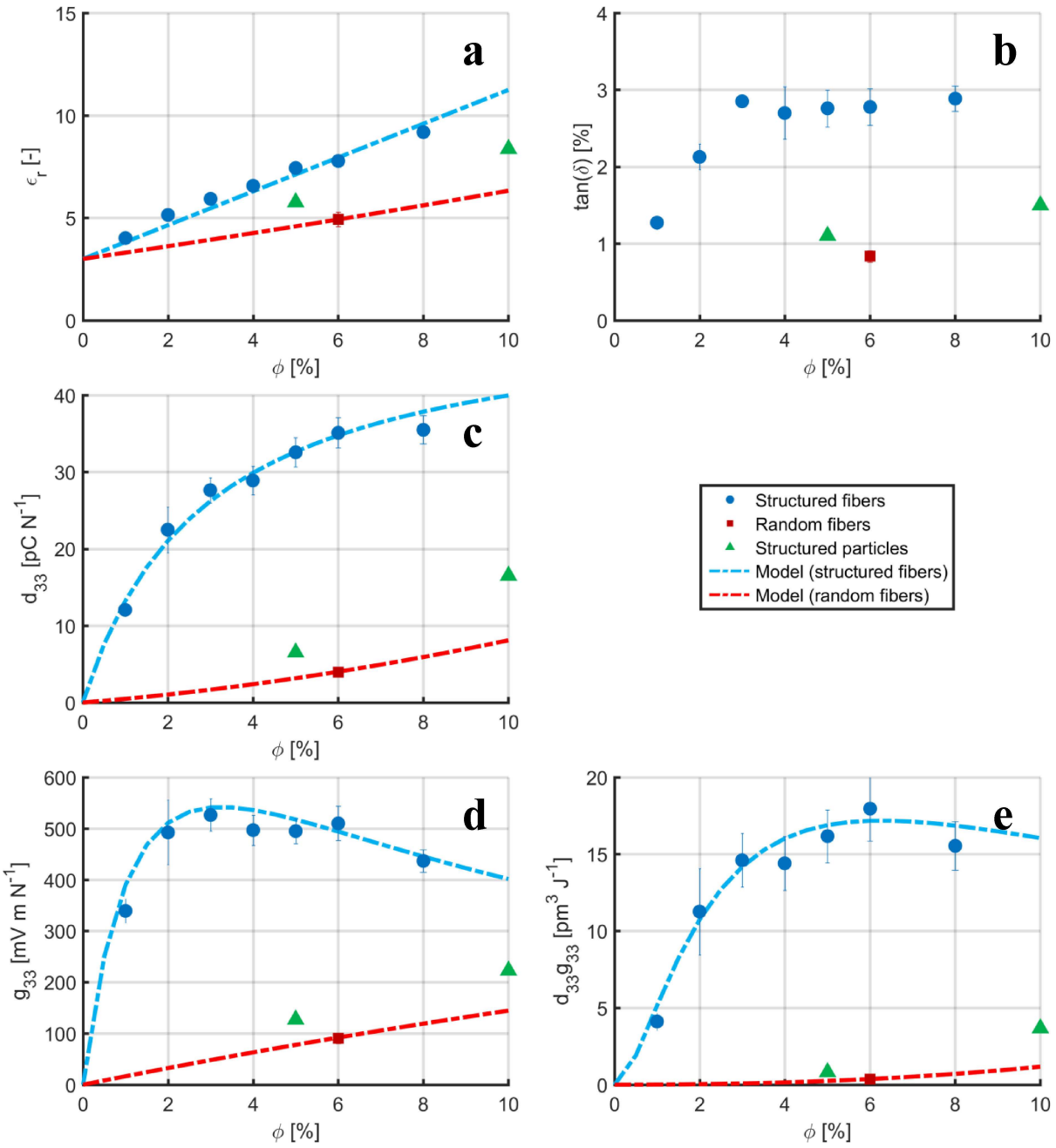

Figure 4. Piezoelectric- and dielectric constants of random 0–3 and structured quasi 1–3 KNLN/PDMS fiber composites as a function of KNLN volume fraction, φ. Blue circles refer to structured composites and red squares refer to random composites. a) The relative dielectric constant, ε_r, b) the dielectric loss, $tan(\delta)$, c) the piezoelectric charge coefficient, d_{33}, d) the piezoelectric voltage coefficient, g_{33}, e) the stress energy density, $d_{33}g_{33}$. For comparison, reported data of quasi 1–3 particle KNLN/PDMS composites are included as the green triangles.[25] The dash-dotted lines are a guide for the eye, calculated with the same models as used in Figure 1.

To verify the high value of $d_{33}g_{33}$, obtained for the aligned KNLN/PDMS fiber composite, we measured the output energy under sinusoidal mechanical excitation in a recently developed piezometer system.[10] The output energy is subsequently compared to that of state-of-the-art ceramic, PZT507,[39] measured under identical conditions.

The electrical output of an energy harvester increases linearly with the mechanical input energy. This input energy strongly depends on the mechanical boundary conditions. The differences between a clamped disc, a bimorph cantilever, unimorph diaphragms or cymbal transducer can easily differ by many orders of magnitude. Here we measured the stored electrical energy of different material classes in the simple boundary condition of a clamped disk. We stress that this is experimentally the only way to reliably compare a variety of piezoelectric materials under identical conditions. However, we note that this clamped condition is the least efficient at transferring the applied load into elastic strain energy.

Table 1. Piezoelectric coefficients of representative piezoelectric materials, ranked on the value of $d_{33}g_{33}$.

Piezoelectric Material	Matrix Material	Connectivity	φ [%]	d_{33} [pC N^{-1}]	g_{33} [mV m N^{-1}]	$d_{33}g_{33}$ [pm^3 J^{-1}]	Reference
PZT507		Bulk	100	875	25	21.9	This work[a)]
Structured KNLN fibers	PDMS	Quasi 1–3	6	35	510	17.9	This work
PT-BFMn	Epoxy	0–3	65	65	230	15.0	[37]
PZT pillars	Epoxy	1–3	48	475	29	13.8	[38]
PZT5A4		Bulk	100	460	28	12.9	[39]
Structured PZT fibers	PU	Quasi 1–3	5	27	277	7.5	[32]
PVDF		Bulk	100	23	220	5.1	[40]
Structured KNLN particles	PDMS	Quasi 1–3	10	17	220	3.7	[25]
Structured KNLN particles	Epoxy	Quasi 1–3	10	20	180	3.6	[24]
KNN		Bulk	100	120	27	3.2	[41]
$BaTiO_3$		Bulk	100	191	11	2.1	[13]
Structured PZT particles	Epoxy	Quasi 1–3	20	10	70	0.7	[21]

[a)] Sintered ceramic disks obtained from CeramTec, Ruabon, UK.

The piezometer system is schematically depicted in Figure 5a. The metallized capacitor is placed between two rounded anvils. Rounded anvils are used with a radius of 1.6 mm, identical to the anvils used in the Berlincourt measurement. The PZT507 and KNLN/PDMS samples have a similar surface area of 50 mm^2 and a similar thickness of 1 mm. The diameter of the anvils is identical to the diameter of the composites. An inductive voice coil supplies a static force of 10 N and a dynamic force of 3 N peak-to-peak, at a frequency of 1 Hz, shown in Figure 5b.

The short circuit current, I_{SC}, is measured using an ultra-low noise amplifier that virtually shorts the sample. The short circuit current is presented in Figure 5c. The current is the derivative of the mechanical force, which explains the observed phase shift between Figure 5b and 5c. The short circuit current scales with the value of d_{33}, which explains the higher current of PZT507 compared to KNLN/PDMS. The open circuit voltage, V_{OC}, is measured with an electrometer, and is presented as a function of time in Figure 5d. The voltage is the second derivative of the applied mechanical force, which for a sinusoidal excitation is equal to the original waveform. The output voltage scales with g_{33}, and therefore, a higher voltage is observed for the KNLN/PDMS. The stored electric energy per unit volume, U_{open}, is calculated from the open circuit voltage by:

$$U_{open} = \frac{C_p V_{oc}^2}{2At} \tag{2}$$

where C_p is the sample capacitance, A the electrode area and t the thickness. The stored electrical energy is presented as a function of time in Figure 5e and 5f, for KNLN/PDMS and PZT507, respectively. From U_{open}, the value of $d_{33}g_{33}$ can be derived, which perfectly agrees with the values presented in Figure 4. As U_{open} depends on V_{oc}^2, it oscillates at double the applied frequency. This is as expected from the comparable values of $d_{33}g_{33}$, the stored electrical energy for KNLN/PDMS is comparable to that of PZT507.

We note that the energy density is low, only in the range of nW cm^{-3}, due to the fact that the sample is mechanically clamped. However, in order to prevent any ambiguous interpretation, we carefully measured the stored energy in our KNLN/PDMS composite materials and PZT under exactly identical conditions. More importantly, in order to prevent any ambiguous interpretation, we carefully measured the stored energy in our KNLN/PDMS composite materials and PZT ceramics under exactly identical conditions. Therefore we can directly compare these two material systems for energy harvesting application. We show that the under identical clamped conditions, a similar output energy is measured for KNLN/PDMS fiber composites and PZT ceramics. This similarity demonstrates that piezoelectric composites can be a worthwhile alternative for state-of-the-art piezoelectric ceramic materials in vibrational energy harvesters.

5. Conclusion

We fabricated quasi 1–3 aligned KNLN ceramic fibers in a PDMS matrix. The fibers were aligned by dielectrophoresis with an orientational order parameter between 0.6 and 0.9. The piezoelectric and dielectric constants were fully characterized as a function of fiber volume fraction. The figure of merit for materials to be applied in vibrational energy harvesters is $d_{33}g_{33}$. Here we demonstrate for the KNLN/PDMS composites values approaching 18 pm^3 J^{-1}. This relatively high value is due to the alignment of fibers, instead of particles, leading to a strongly reduced inter-particle distance. The value of $d_{33}g_{33}$ is comparable to that of state-of-the-art PZT ceramics. Using a sensitive piezometer system, the stored electrical energy is measured under sinusoidal mechanical excitation. Under identical clamped conditions, a similar output energy is measured for KNLN/PDMS and PZT, as expected from the similar value of $d_{33}g_{33}$. This unambiguously demonstrates that environmentally friendly, lead-free, mechanically compliant materials can replace state-of-the-art brittle and damage-sensitive ceramics in piezoelectric vibrational energy harvesters.

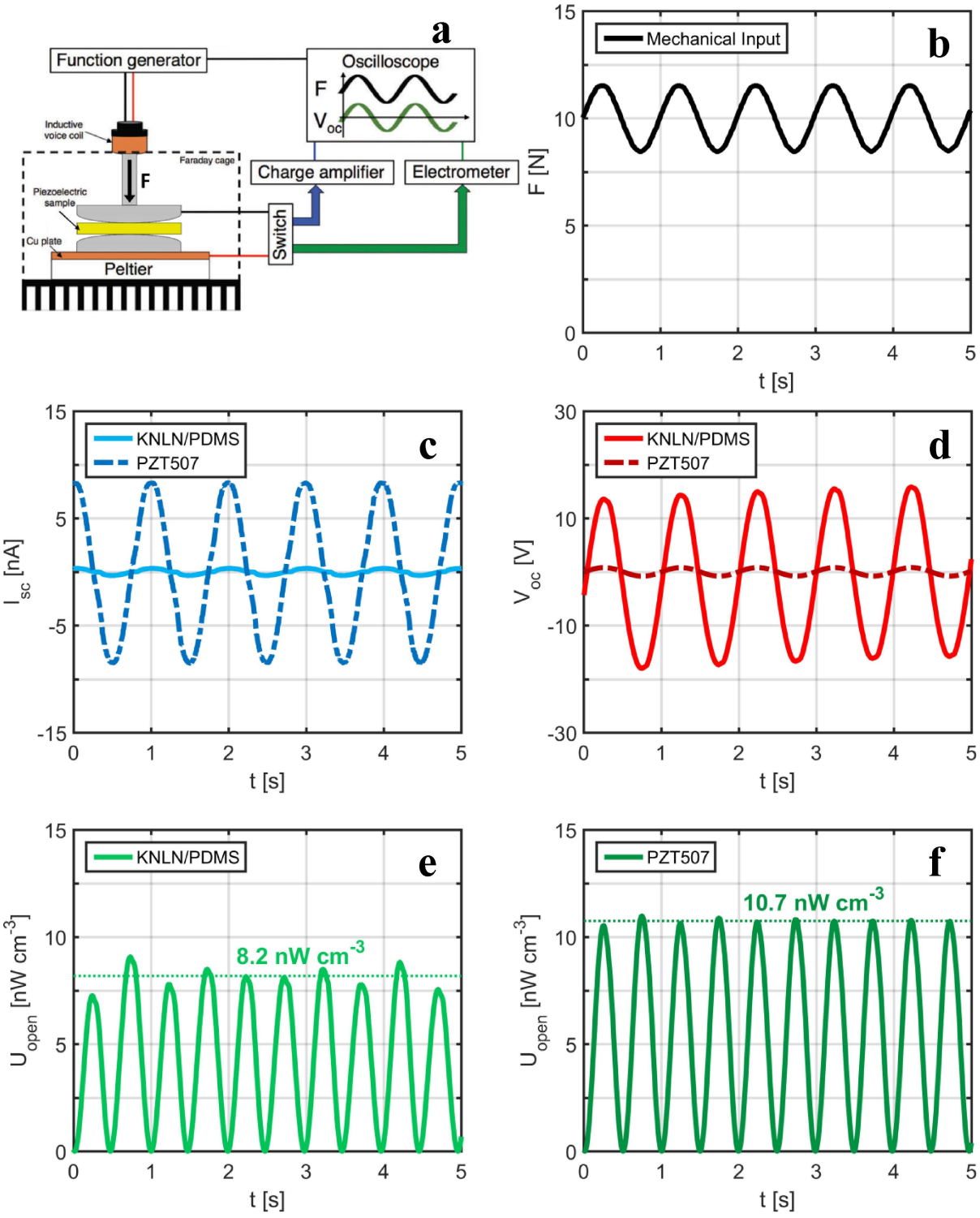

Figure 5. Electrical response to a mechanical input of KNLN/PDMS and PZT507, both having a thickness of 1 mm and an area of 50 mm^2, measured using a specifically designed piezometer system. a) Schematic representation of the piezometer system,[10] b) the mechanical input, *F*, c) the short circuit current, I_{sc}, d) the open circuit voltage, V_{oc}, and the stored electrical energy, U_{open}, of e) KNLN/PDMS and f) PZT507, respectively.

Experimental Section

Optical micrographs were used to determine the aspect ratio distribution of the KNLN fibers. A field emission scanning electron microscope (SEM) (JEOL, JSM-7500F, Nieuw Vennep, the Netherlands) was used to determine the fiber thickness and fiber morphology. Optical micrographs of the composite cross sections were used to determine the fiber alignment. Per sample set, six different cross sections were examined and, using ImageJ software, the orientation of the fiber chains were analyzed. The piezoelectric charge coefficient, d_{33}, was measured with a Berlin-

court-type piezometer on poled capacitors (PM300, Piezotest, London, UK). Rounded anvils are used with a radius of 1.6 mm. A static force of 10 N was applied, under a 0.25 N peak-to-peak sinusoidal excitation at 110 Hz. We note that the extracted value of d_{33} depends on the boundary conditions, such as the sample aspect ratio.[42] Here all measurements have been performed under identical conditions using rounded anvils. Therefore the extracted values of d_{33} can be directly compared, resulting in a reliable material comparison. The capacitance and dielectric loss were measured at 1 kHz and 1 V with an Agilent 4263B LCR meter (Santa Clara, CA, USA). The relative dielectric constant, ε_r, measured under zero stress, was derived from the capacitance.

Conflict of interest

The authors declare no conflict of interest.

Keywords: alkaline niobates · dielectrophoresis · energy harvesting · quasi 1–3 composites · lead-free piezoelectric materials

[1] M. Wahbah, M. Alhawari, B. Mohammad, H. Saleh, M. Ismail *IEEE J. Emerg. Selec. Top. Circ. Syst.* **2014**, *4*, 354.
[2] C. R. Bowen, H. A. Kim, P. M. Weaver, S. Dunn, *Energy Environ. Sci.* **2014**, *7*, 25.
[3] H. Abdi, N. Mohajer, S. Nahavandi, *J. Intell. Mater. Syst. Struct.* **2014**, *25*, 923.
[4] C. H. Wong, Z. Dahari, A. A. Manaf, M. A. Miskam, *J. Electron. Mater.* **2015**, *44*, 13.
[5] S. P. Beeby, M. J. Tudor, N. M. White, *Meas. Sci. Technol.* **2006**, *17*, R175
[6] H. A. Sodano, D. J. Inman, G. Park, *Shock Vib. Dig.* **2004**, *36*, 197.
[7] K. A. Cook-Chennault, N. Thambi, M. A. Bitetto, E. B. Hameyie *Bullet. Sci. Tech. Soc.* **2008**, *28*, 496.
[8] H. Li, C. Tian, Z. D. Deng, *Appl. Phys. Rev.* **2014**, *1*, 041301.
[9] R. A. Islam, S. Priya, *Appl. Phys. Lett.* **2006**, *88*, 032903.
[10] D. B. Deutz, J. Pascoe, B. Schelen, S. van der Zwaag, D. M. de Leeuw, P. Groen, *Mater. Horiz.*, DOI: 10.1039/c8mh00097b.
[11] J. Rödel, K. G. Webber, R. Dittmer, W. Jo, M. Kimura, D. Damjanovic, *J. Eur. Ceram. Soc.* **2015**, *35*, 1659.
[12] T. R. Shrout, S. J. Zhang, *J. Electroceram.* **2007**, *19*, 111.
[13] T. Rödig, A. Schönecker, G. Gerlach, *J. Am. Ceram. Soc.* **2010**, *93*, 901.
[14] T. Furukawa, *IEEE Trans. Electr. Insul.* **1989**, *24*, 375.
[15] I. Katsouras, K. Asadi, M. Li, T. B. van Driel, K. S. Kjær, D. Zhao, T. Lenz, Y. Gu, P. W. Blom, D. Damjanovic, M. M. Nielsen, D. M. de Leeuw, *Nat. Mater.* **2015**, *15*, 78.
[16] C. Dias, D. K. Das-Gupta, Y. Hinton, R. J. Shuford, *Sens. Actuators A* **1993**, *37*, 343.
[17] A. Peláiz-Barranco, P. Marin-Franch, *J. Appl. Phys.* **2005**, *97*, 34104.
[18] G. Sa-Gong, A. Safari, S. J. Jang, R. E. Newnham, *Ferroelectr. Lett. Sect.* **1986**, *5*, 131.
[19] R. E. Newnham, D. P. Skinner, L. E. Cross, *Mater. Res.* **1978**, *13*, 525.
[20] T. Yamada, T. Ueda, T. Kitayama, *J. Appl. Phys.* **1982**, *53*, 4328.
[21] D. A. van den Ende, B. F. Bory, W. A. Groen, S. van der Zwaag, *J. Appl. Phys.* **2010**, *107*, 024107.
[22] D. Y. Wang, K. Li, H. L. W. Chan, *Sens. Actuators A* **2004**, *114*, 1.
[23] A. Abrar, D. Zhang, B. Su, T. W. Button, K. J. Kirk, S. Cochran, *Ultrasonics* **2004**, *42*, 479.
[24] N. K. James, D. B. Deutz, R. K. Rose, S. van der Zwaag, P. Groen, *J. Am. Ceram. Soc.* **2016**, *99*, 3957.
[25] D. B. Deutz, N. T. Mascarenhas, S. van der Zwaag, W. A. Groen, *J. Am. Ceram. Soc.* **2017**, *100*, 1.
[26] T. Bhimansankaram, S. V. Suryanarayana, G. Prasad *Curr. Sci.* **1998**, *74*, 967.
[27] F. Carpi, D. De Rossi, *IEEE Trans. Dielectr. Electr. Insul.* **2005**, *12*, 835.
[28] T. Furukawa, K. Ishida, E. Fukada, *J. Appl. Phys.* **1982**, *53*, 4328.
[29] C. P. Bowen, R. E. Newnham, C. A. Randall, *J. Mater. Res.* **1998**, *13*, 1.
[30] M. C. Araújo, C. M. Costa, S. Lanceros-Méndez, *J. Non-Cryst. Solids* **2014**, *387*, 6.
[31] H. Khanbareh, S. van der Zwaag, W. A. Groen, *Smart Mater. Struct.* **2014**, *23*, 105030.
[32] D. A. van den Ende, S. E. van Kempen, X. Wu, W. A. Groen, C. A. Randall, S. van der Zwaag, *J. Appl. Phys.* **2012**, *111*, 124107.
[33] S. A. Wilson, G. M. Maistros, R. W. Whatmore, *J. Phys. D* **2005**, *38*, 2.
[34] N. D. Spencer, J. H. Moore, *Encyclopedia of chemical physics and physical chemistry*, Institute of Physics, Bristol, UK **2001**.
[35] M. A. Gutiérrez, H. Khanbareh, S. van der Zwaag, *Comput. Mater. Sci.* **2016**, *112*, 139.
[36] D. B. Deutz, N. T. Mascarenhas, S. van der Zwaag, W. A. Groen, *Ferroelectrics* **2017**, *515*, 68.
[37] K. Han, A. Safari, R. E. Riman, *J. Am. Ceram. Soc.* **1991**, *74*, 1699.
[38] Datasheet Smart Materials 1–3 Composites, https://www.smart-material.com/Datasheets-13 K.html, accessed 16–04-2018.
[39] Datasheet Ceramtec PZT5 A/507, https://www.ceramtec.com/ceramic-materials/soft-pzt/, accessed 16–04-2018.
[40] Piezotech, Company Literature, *Piezoelectric Films Technical Information*, Hésingue, France **2012**.
[41] H. Du, Z. Li, F. Tang, S. Qu, Z. Pei, W. Zhou, *Mater. Sci. Eng. B* **2006**, *131*, 83.
[42] A. Barzegar, D. Damjanovic, N. Setter *IEEE Trans. Ultrason. Ferroel. Freq. Contr.* , **2004**, *51*, 262–270.

Manuscript received: May 18, 2018
Revised manuscript received: August 7, 2018
Accepted manuscript online: August 10, 2018
Version of record online: November 23, 2018

